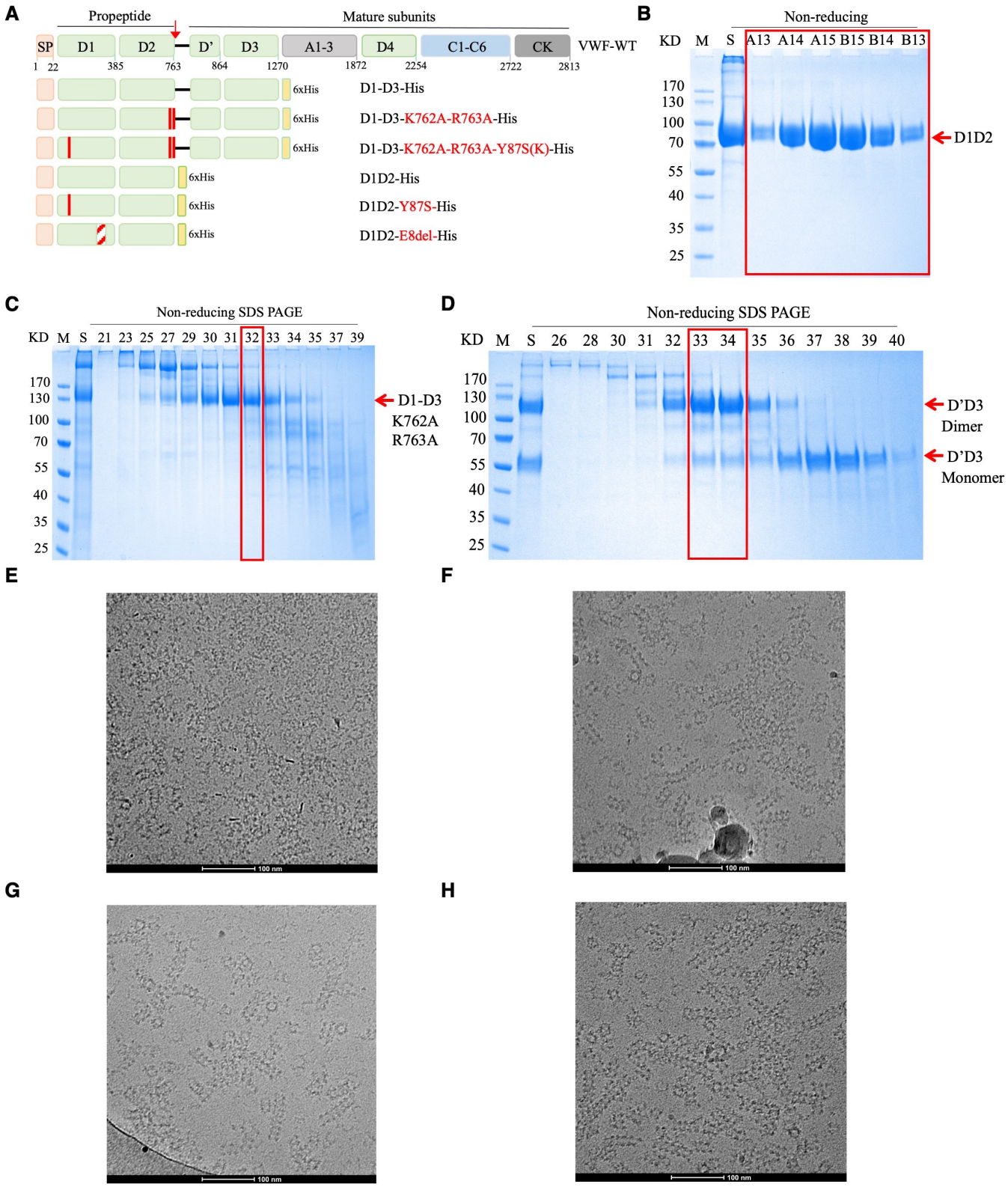

Supplementary Figure S1: Protein sample preparation. A. A diagram showing the different expression constructs used in this study. The HEK293 suspension cell were transfected with D1D2-His variants, D1-D3-His or D1-D3-K762A-R763A-His etc. expression plasmid respectively. The expression medium containing these proteins was first purified by Ni-Chelating followed by an anion exchange column, and finally purified by a Superdex200pg 16/60GL column (GE). The fractions from the final gel filtration step were analyzed by SDS-PAGE (**B-D)** respectively. The purified protein samples (indicated by red box) including D1D2 and D'D3 dimer were used in Cryo-EM analysis. **E-H.** The D1D2 and D'D3 dimer were mixed and incubated for 8min, 20min, 40min and over night at 4°C respectively, and analyzed by Cryo-EM (scale bar = 100 nm).

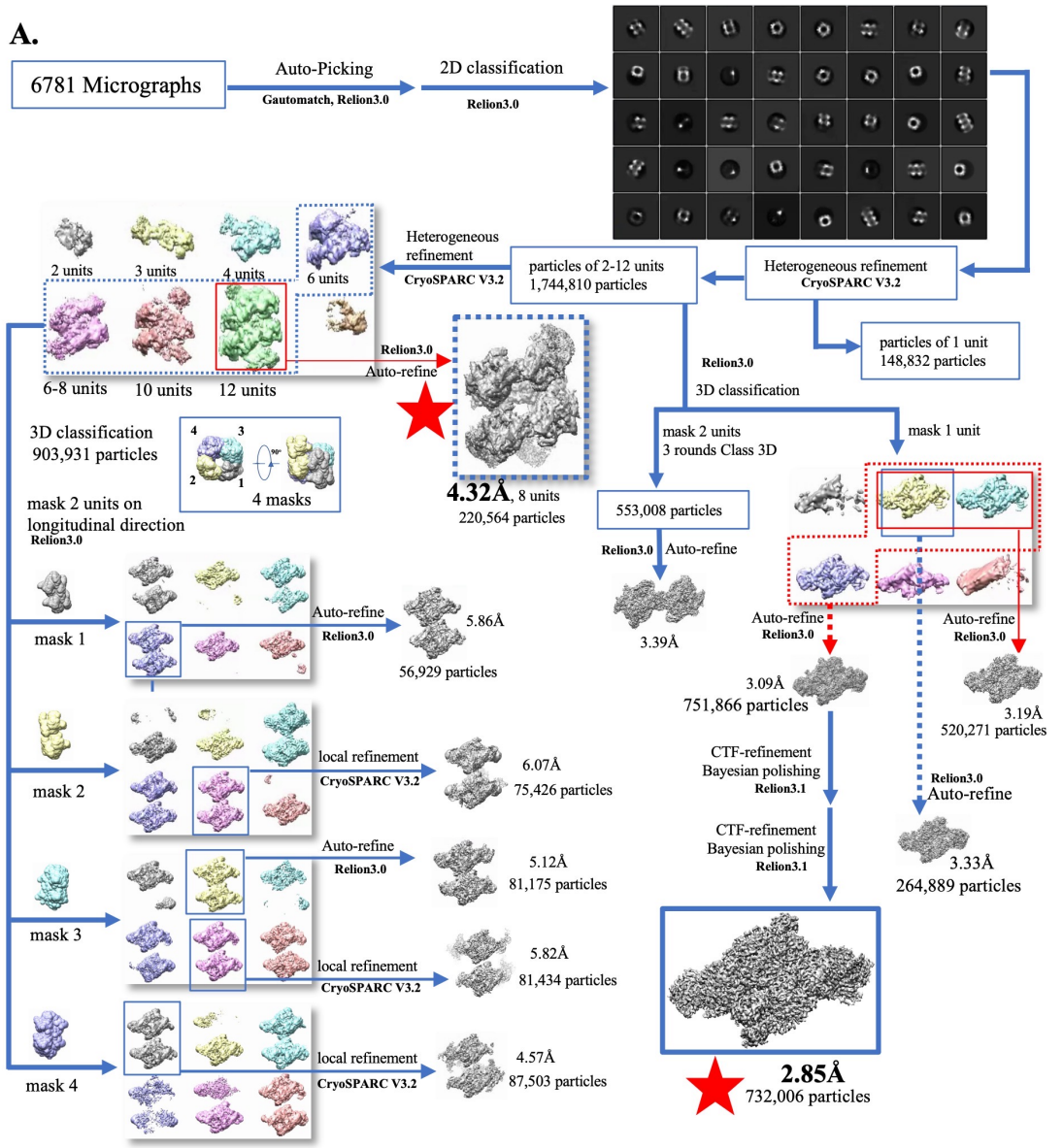
A.
6781 Micrographs
Auto-Picking
Gautomatch, Relion3.0
2D classification
Relion3.0
Heterogeneous refinement
CryoSPARC V3.2
particles of 2-12 units
1,744,810 particles
Heterogeneous refinement
CryoSPARC V3.2
particles of 1 unit
148,832 particles
2 units
3 units
4 units
6 units
6-8 units
10 units
12 units
Relion3.0
Auto-refine
4.32Å, 8 units
220,564 particles
Relion3.0
3D classification
3D classification
903,931 particles
4 masks
mask 2 units on
longitudinal direction
Relion3.0
mask 2 units
3 rounds Class 3D
mask 1 unit
553,008 particles
Relion3.0
Auto-refine
3.39Å
mask 1
Auto-refine
Relion3.0
5.86Å
56,929 particles
Auto-refine
Relion3.0
3.09Å
751,866 particles
Auto-refine
Relion3.0
3.19Å
520,271 particles
mask 2
local refinement
CryoSPARC V3.2
6.07Å
75,426 particles
CTF-refinement
Bayesian polishing
Relion3.1
Relion3.0
Auto-refine
mask 3
Auto-refine
Relion3.0
5.12Å
81,175 particles
CTF-refinement
Bayesian polishing
Relion3.1
3.33Å
264,889 particles
local refinement
CryoSPARC V3.2
5.82Å
81,434 particles
mask 4
local refinement
CryoSPARC V3.2
4.57Å
87,503 particles
2.85Å
732,006 particles

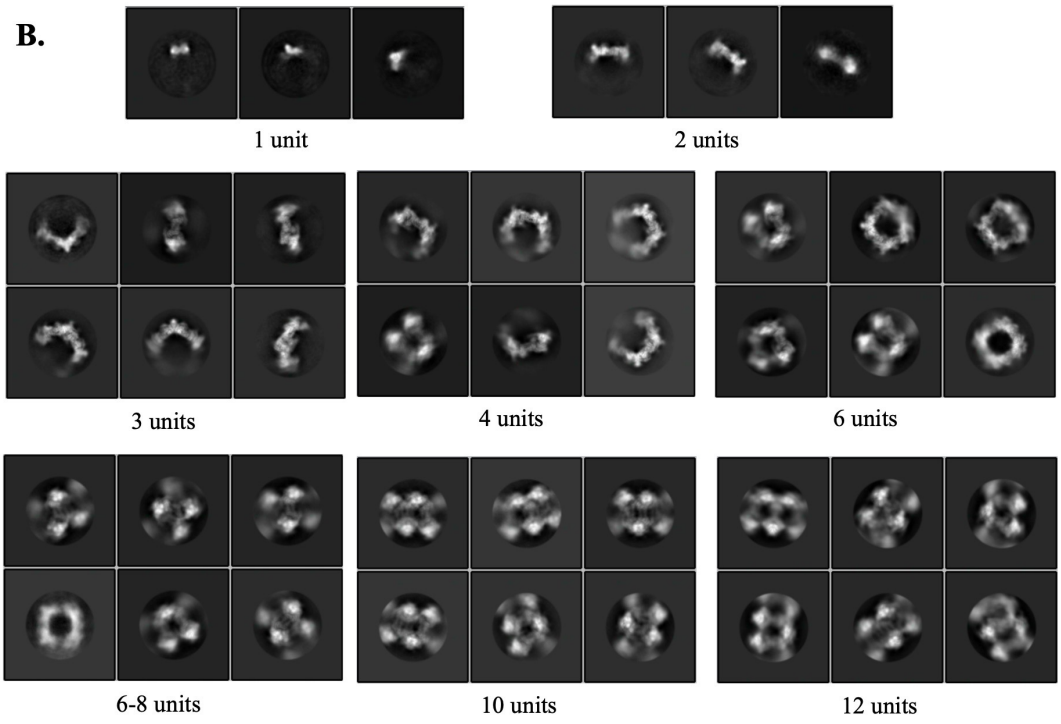
B.
1 unit
2 units
3 units
4 units
6 units
6-8 units
10 units
12 units

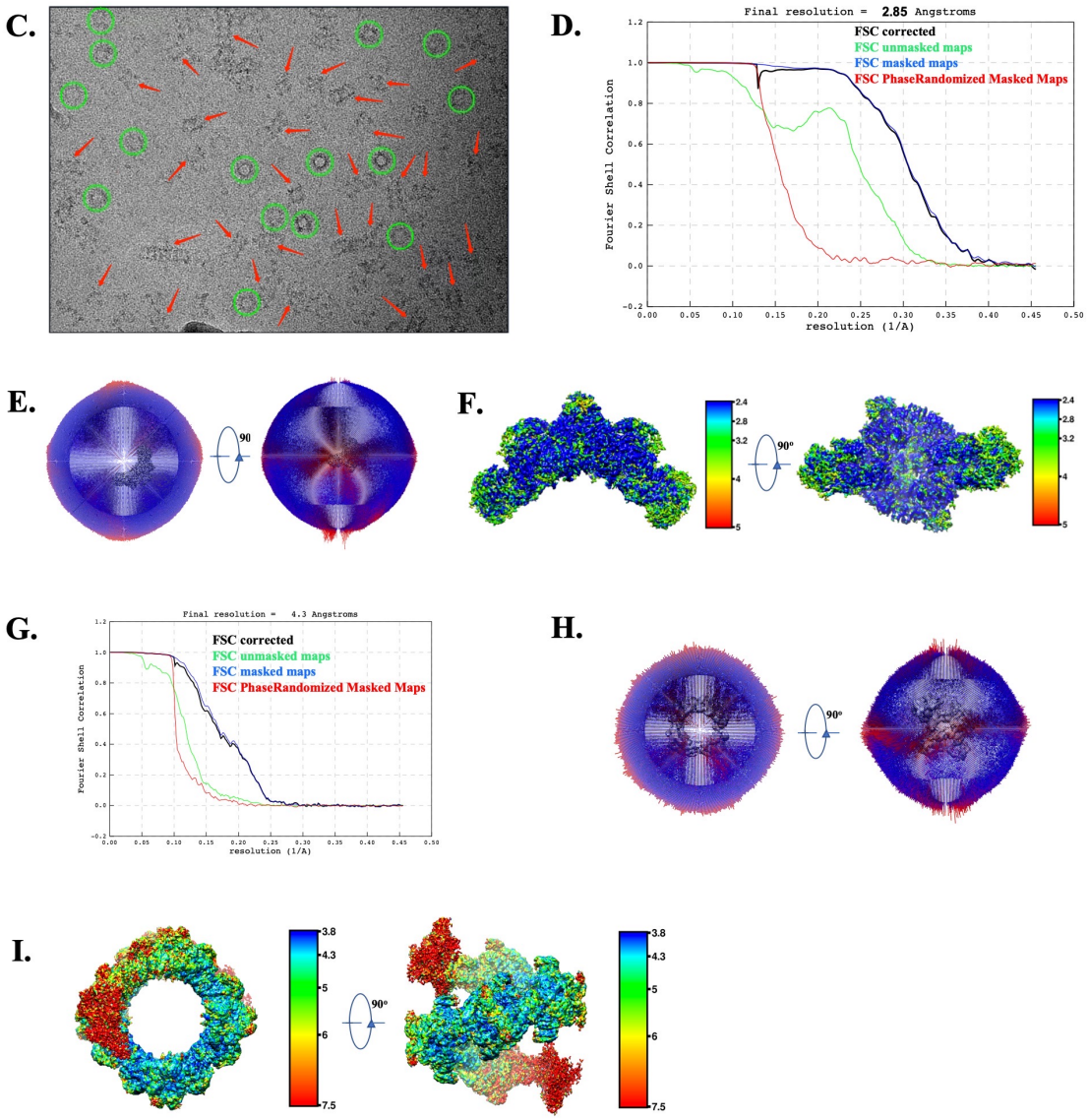

Supplementary Figure S2: Cryo-EM analysis of the VWF D1D2-D'D3 dimer mixture (incubate 8 min, used for determining the final 1-unit and 8-units structure of the VWF). A. Flowchart for cryo-EM data processing, the 2.85Å 1 unit map indicated by blue box and red five-pointed star was analyzed in (**D-F**), the 4.32Å VWF tube map indicated by blue dotted line and red five-pointed star was analyzed in (**G-I**). **B.** Representative 2D class averages. Particles belong to for different classes (from 1unit to 12 units, labeled under each 2D class average) were selected from CryoSPARC Heterogeneous Refinement in (**A**). **C.** A representative cryo-EM micrograph. Top view particles were picked with green cycles, diameter=350Å; several side view particles or filament were pointed out with red arrows. **D.** The gold-standard Fourier shell correlation (FSC) curves for the 2.85Å 1 unit map in (**A**). **E.** Angular distribution of cryo-EM particles used for final structural refinement of the 2.85Å 1 unit map in (**A**). **F.** Local resolution map for the 3D EM reconstruction of the 2.85Å 1 unit map in (**A**). **G.** The gold-standard Fourier shell correlation (FSC) curves for the 4.32Å VWF tube map in (**A**). **H.** Angular distribution of cryo-EM particles used for final structural refinement of the 4.32Å VWF tube map in (**A**). **I.** Local resolution map for the 3D EM reconstruction of the 4.32Å VWF tube map in (**A**).

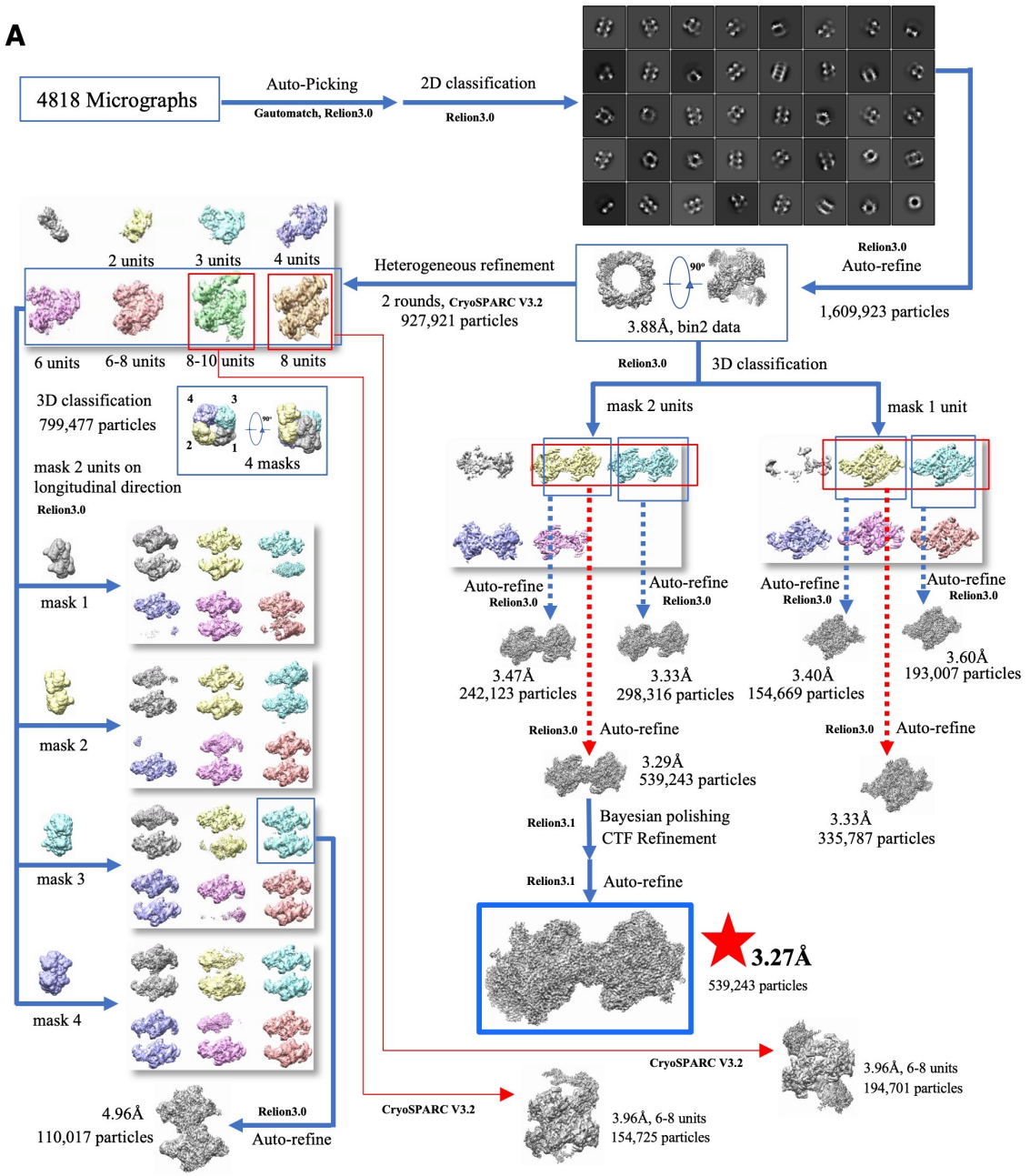
A
4818 Micrographs
Auto-Picking
Gautomatch, Relion3.0
2D classification
Relion3.0
Relion3.0
Auto-refine
1,609,923 particles
3.88Å, bin2 data
Heterogeneous refinement
2 rounds, CryoSPARC V3.2
927,921 particles
2 units
3 units
4 units
6 units
6-8 units
8-10 units
8 units
Relion3.0
3D classification
mask 2 units
mask 1 unit
3D classification
799,477 particles
mask 2 units on
longitudinal direction
4 masks
Relion3.0
mask 1
mask 2
mask 3
mask 4
Auto-refine
Relion3.0
3.47Å
242,123 particles
Auto-refine
Relion3.0
3.33Å
298,316 particles
Auto-refine
Relion3.0
3.40Å
154,669 particles
Auto-refine
Relion3.0
3.60Å
193,007 particles
Relion3.0
Auto-refine
3.29Å
539,243 particles
Relion3.0
Auto-refine
3.33Å
335,787 particles
Relion3.1
Bayesian polishing
CTF Refinement
Relion3.1
Auto-refine
3.27Å
539,243 particles
CryoSPARC V3.2
3.96Å, 6-8 units
194,701 particles
CryoSPARC V3.2
3.96Å, 6-8 units
154,725 particles
4.96Å
110,017 particles
Relion3.0
Auto-refine
B
1 unit (top) and 2 units (bottom)
3 units
4 units
6 units
8 units
10 units

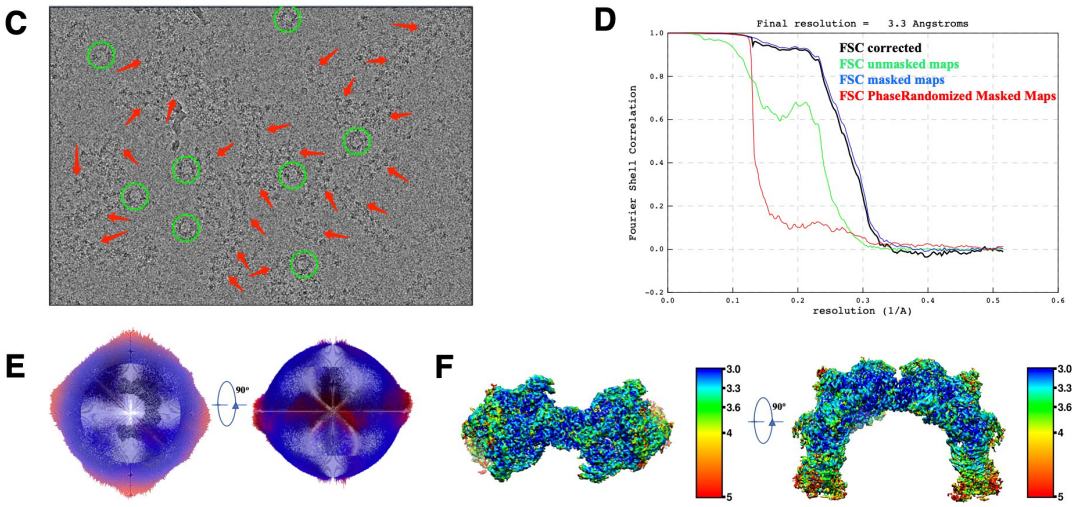

Supplementary Figure S3: Cryo-EM analysis of the VWF D1D2-D'D3 dimer mixture (incubated overnight, used for determining the final 2-units structure of the VWF) . A. Flowchart for cryo-EM data processing, the 3.27Å 2-units map indicated by blue box and red five-pointed star was analyzed in (**D-F**). **B.** Representative 2D class averages. Particles belong to for different classes (from 1unit to 10 units, labeled under each 2D class average) were selected from CryoSPARC Heterogeneous Refinement in (**A**). **C.** A representative cryo-EM micrograph. Top view particles were picked with green cycles, diameter=350Å; several side view particles or filament were pointed out with red arrows. **D.** The gold-standard Fourier shell correlation (FSC) curves for the 3.27Å 2-units map in (**A**). **E.** Angular distribution of cryo-EM particles used for final structural refinement of the 3.27Å 2-units map in (**A**). **F.** Local resolution map for the 3D EM reconstruction of the 3.27Å 2-units map in (**A**).

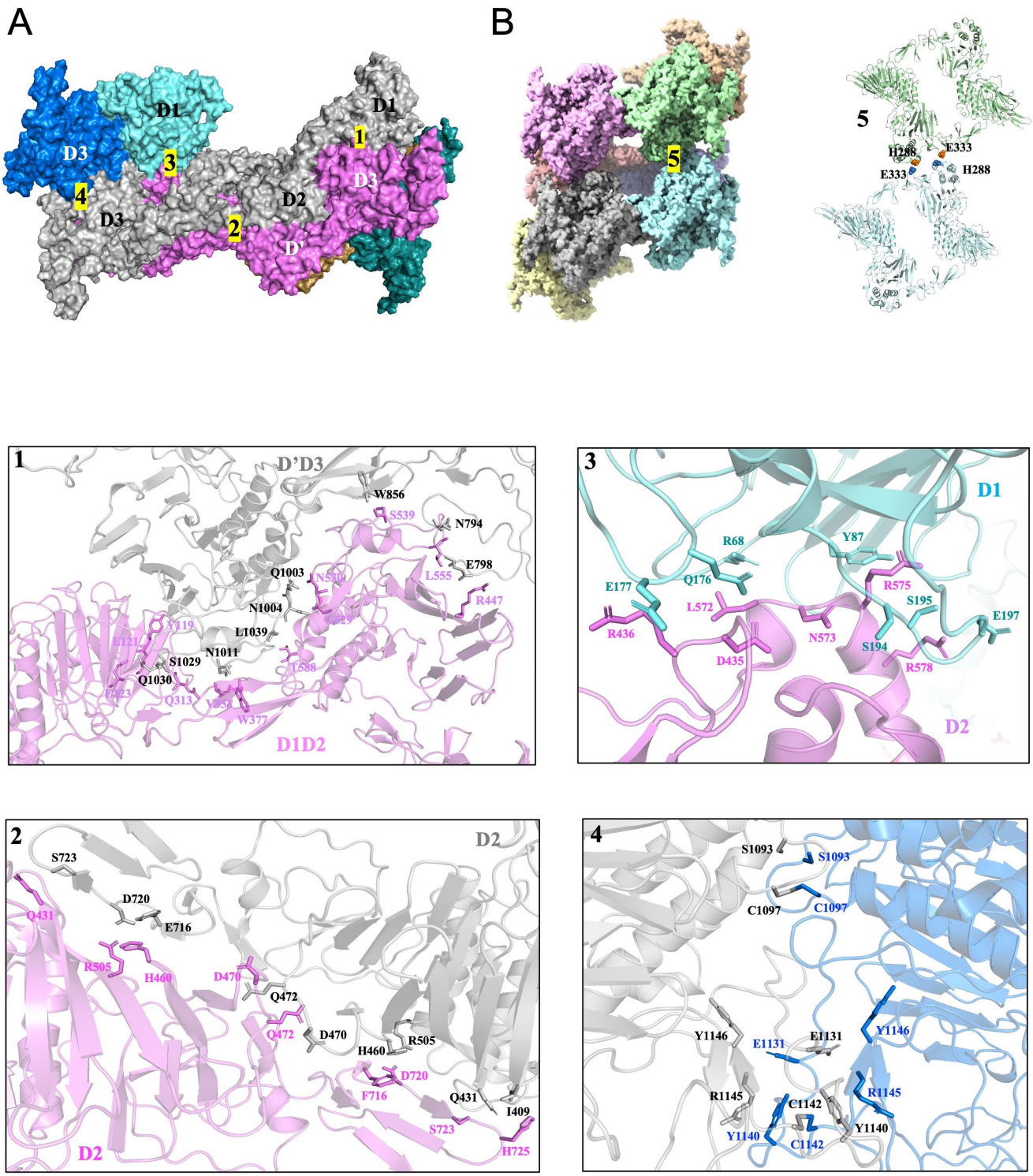

Supplementary Figure S4: Intermolecular binding interfaces of VWF tubules. **A.** The Cryo-EM structure of tubule with two repeating units. **B.** The Cryo-EM structure of tubule with 8 repeating units. The interfaces are labeled and shown as follows: 1. The D1D2: D'D3 binding interface. The D' region undergoes large conformational changes upon binding of D2 when compared with its monomeric crystal structure. His831 in D' upon protonation could form ionic interaction with Glu 543 of D2. 2. The D2:D2 interface. 3. The D1:D2 interface. 4. The dimeric DiD3 interface. 5. The D1:D1 interface along the tubule extension axis. Residues involved are shown in sticks of spheres. The two D1D2D'D3 chains colored grey and purple respectively (**A**).

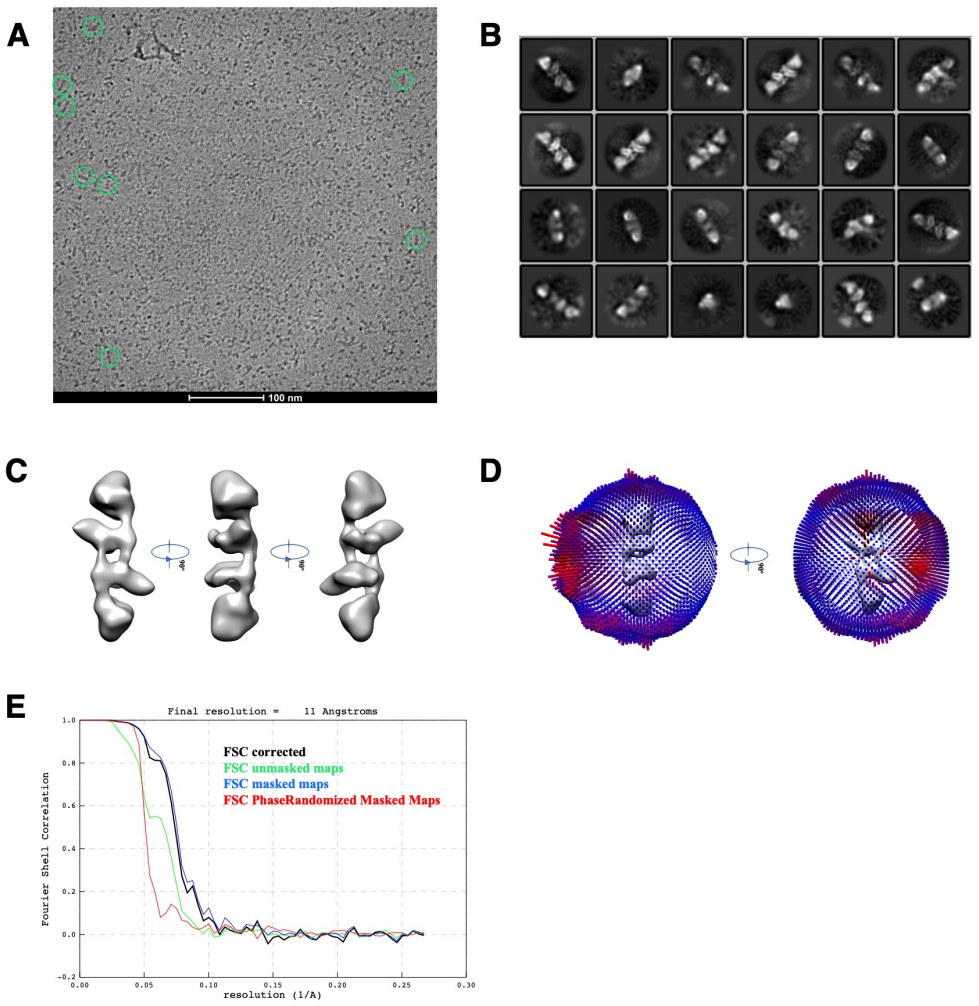

Supplementary Figure S5: Cryo-EM analysis of the VWF D1D2 dimer. A. A representative cryo-EM micrograph. Several particles were picked with green cycles, scale bar = 100 nm. **B.** Representative 2D class averages. **C.** 3D EM reconstruction map of D1D2 dimer. **D.** Angular distribution of cryo-EM particles used for final structural refinement. **E.** The gold-standard Fourier shell correlation (FSC) curves.

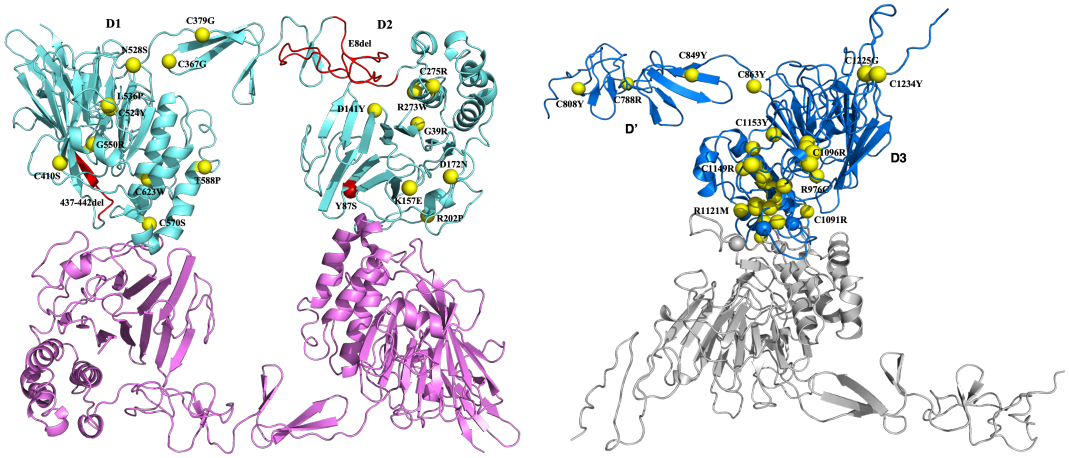

Type 2A VWD mutations	Structural analysis	Disrupted steps
G39R[1]	located in VWD1 module; disrupted the local packing between VWD1 and C8-1 modules, and destabilized the D1:D2 interface	iii
D141N[2]	located in VWD1 module; disrupted the D141-R273 salt bridge and destabilized the local packing between VWD1 and C8-1 modules	iii
K157E[3]	located in VWD1 module; formed a new potential salt bridge with K67 and disrupted the D1:D2 interface	iii
D172N[4]	located in VWD1 module; cause an extra glycosylation site in N172 and destabilized the D1:D2 interface	iii
R273W[5]	located in C8-1 module; disrupted the D141-R273 salt bridge and destabilized the local packing between VWD1 and C8-1 modules	iii
C275R[6]	located in C8-1 module; disrupted the Cys237-Cys275 disulfide bond and destabilized the D1 domain	iii
C379G[7]	located in E1 module; disrupted the Cys370-Cys379 disulfide bond and destabilized the cradle region	ii
F404insNP[8]	located in VWD2 module; disrupted the local packing and destabilized the VWD2 module	i
C410S[9]	located in VWD2 module; disrupted the Cys559-Cys410 disulfide bond and destabilized the D2:D' interface	ii
D437_R442del[10]	located in VWD2 module; disrupted the local packing and destabilized the VWD2 module	i
C524Y[11]	located in VWD2 module; disrupted the Cys388-Cys524 disulfide bond and destabilized local packing between VWD2 and C8-2 modules	i
N528S[12]	located in VWD2 module; disrupted the calcium binding site; cause an extra glycosylation site in N526 and destabilized the VWD2 module; destabilized the D2:D'D3 interface	ii
L536P[13]	located in VWD2 module; disrupted the local packing and destabilized the D2:D'D3 interface	ii
G550R[14]	located in VWD2 module; disrupted the local packing and destabilized the D2:D' interface	ii
C570S[15]	located in C8-2 module; disrupted the Cys613-Cys570 disulfide bond and destabilized local packing between VWD2 and C8-2 modules	i
T588P[16]	located in C8-2 module; disrupted the local packing and destabilized the D2:D'D3 interface	ii
C623W[17]	located in C8-2 module; disrupted the Cys648-Cys623 disulfide bond and destabilized local packing between VWD2 and C8-2 modules	i
G624_A625insG[18]	located in C8-2 module; disrupted the Cys648-Cys623 disulfide bond and destabilized local packing between VWD2 and C8-2 modules	i
C709LfsX3[19]	located in E2 module; disrupted the Cys731-Cys709 disulfide bond and destabilized the D2:D2 interface	i
Y87S[20]	located in VWD1 module; disrupted the Y87-R575 intermolecular interaction and destabilized the D1:D2 interface; see Fig. 3D	iii
R202P[21]	located in VWD1 module; disrupted the R202-Y730 intermolecular interaction and destabilized the D1:D2" interface; see Fig. 3G	iii
R202W[22]	located in VWD1 module; disrupted the R202-Y730 intermolecular interaction and destabilized the D1:D2" interface; see Fig. 3G	iii

1: Journal of Hematology & Oncology 2015; 8:73; **2:** Journal of Hematology & Oncology 2015; 8:73; **3:** Journal of Hematology & Oncology 2015; 8:73; **4:** Medicine2016; 95(11), e3038; **5:** Blood 2000; 96:560-568; **6:** Haemophilia 2008; 14, 549–555; **7:** Journal of Hematology & Oncology 2015; 8:73; **8:** Holmberg et al, 1998; **9:** Haemophilia 2013; 19, e256-e269; **10:** J Thromb Haemost 2009; 7: 641–50; **11:** Clin Chem 2013; 59, 684; **12:** Blood 2010;115(22): 4580-4587; **13:** Thromb Haemost 2014; 112, 96; **14:** Hum Genet 1995; 95:681-686; **15:** Thromb Haemost 2008; 100: 211–216; **16:** Medicine 2016; 95(11), e3038; **17:** Gaucher et al., 1994; **18:** Gaucher et al., 1994; **19:** Gaucher et al., 1994; **20:** Blood 2002; 100:1699-1706; **21:** Hamostaseologie 2009; 29, 143; **22:** J Thromb Haemost 2009; 7:1114-1121

Supplementary Figure S6: Clinically identified type 2A VWD mutations in D1D2 and D'D3. The detailed structural analysis of mutations in D1D2 is summarized in the table.

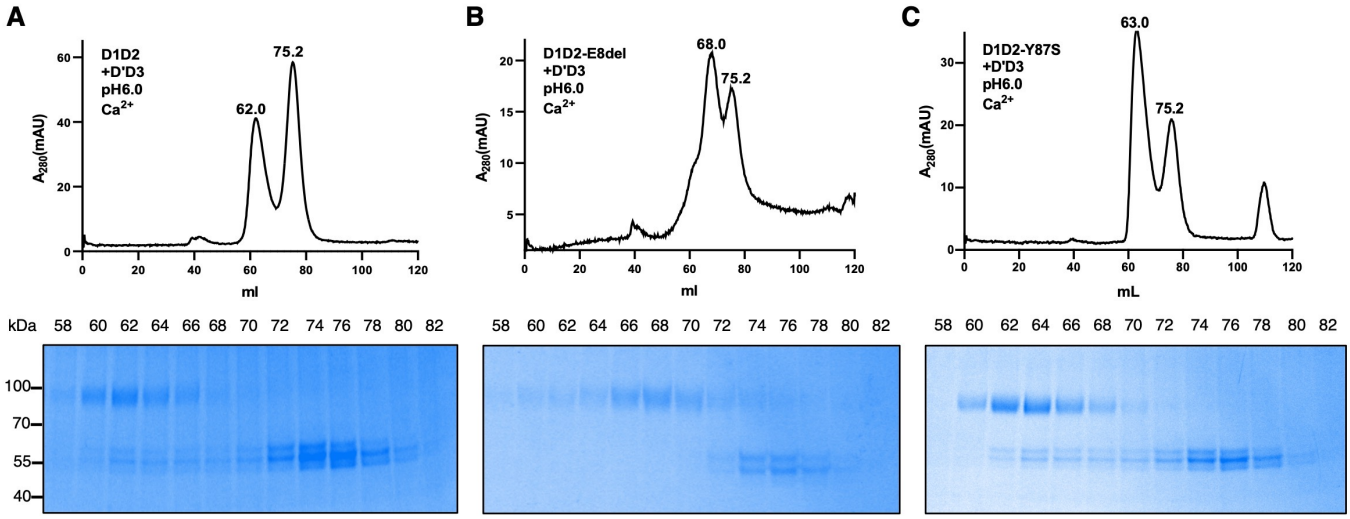

Supplementary Figure S7: Binding interactions between D1D2 and D'D3 monomer assessed by a gel filtration column at pH6 in the presence of calcium. Normal D1D2 (A), D1D2-E8del (B), D1D2-Y87S were mixed with D'D3 monomers respectively and then analyzed by a Superdex200pg gel filtration column with fractions analyzed by SDS-PAGE. Small amount of D'D3 was co-eluted in the peak of normal D1D2 (A) or D1D2-Y87S (C), however, little D'D3 was observed in the peak of D1D2-E8-del (B).

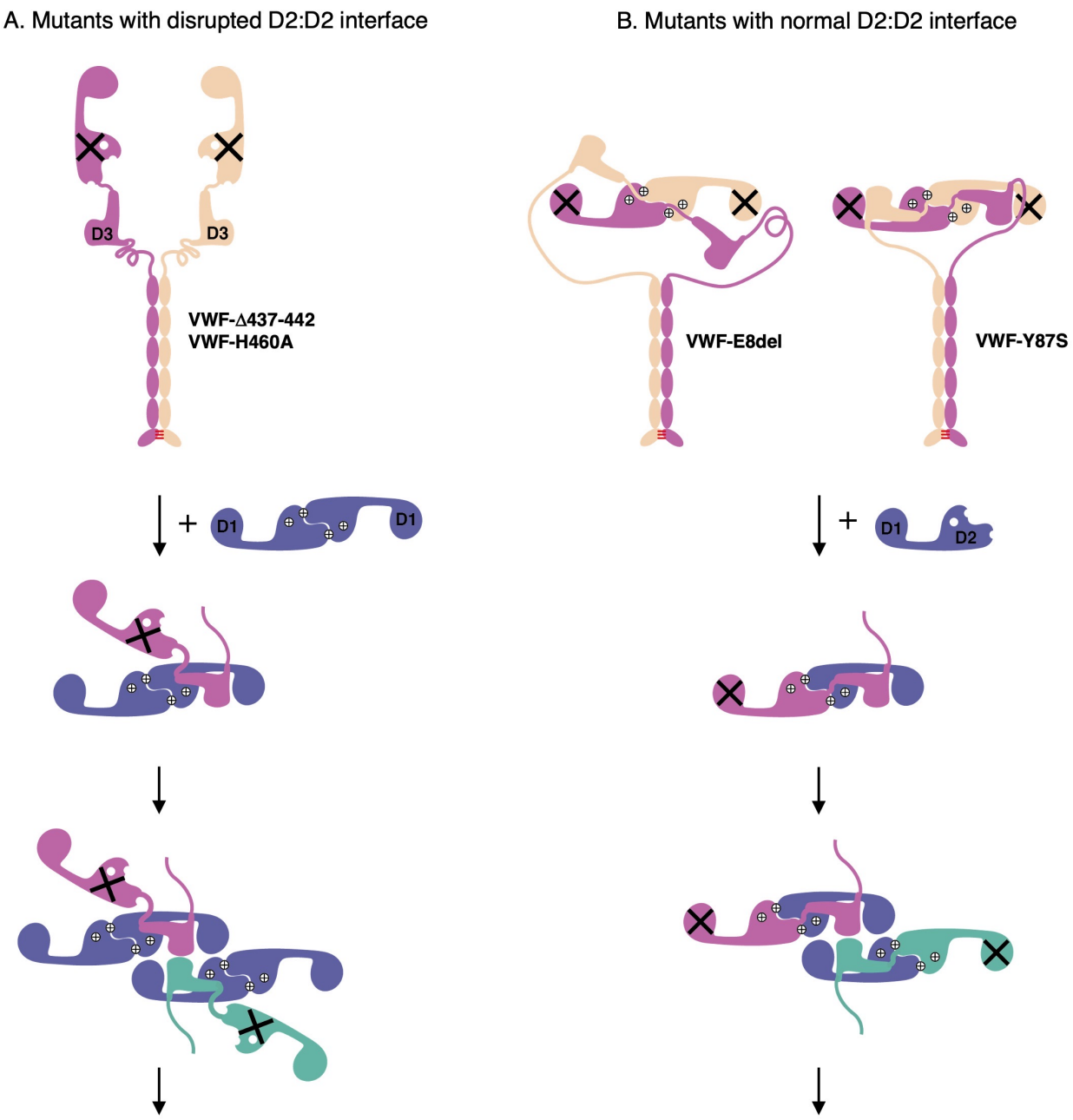

Supplementary Figure S8: The restoration of multimerization of type 2A VWF mutants. A. For VWF mutants with defects in the D2:D2 interface, such as VWF-Δ437-442 and VWF-H460A, their multimerization could be restored by the external D1D2. **B.** Type 2A VWF mutants with normal D2:D2 interfaces, such as VWF-E8del and VWF-Y87S, retain the ability to form closed proVWF dimers. It would require larger amount of external D1D2 to block the closed dimer and subsequently facilitate multimerization of the mutants.

Dataset name	D1D2-D'D3 dimer mixture (8 min)		D1D2-D'D3 dimer mixture (over night)	D1D2 dimer
Grid (Quantifoil, R1.2/1.3)	Au 300mesh		Au 300mesh	Au 300mesh
Data collection and processing				
Voltage (kV)	300		300	200
Electron exposure (e^{-}/Å^2)	50			
Defocus range (μm)	-1.0~-2.0			
Pixel size (Å)	1.0979		0.97	0.936
map	**1 unit**	**Multi units tubule**	**2 units**	
Symmetry imposed	C1			
Final dataset (# of particles)	751,866	751,866	539,243	199,496
Map resolution (Å) $FSC_{0.143}$	**2.85**	**4.32**	**3.27**	11.4
Map-sharpening B factor (Å^2)	-62.0	-141	-92.2	-73.3
Model composition				
Nonhydrogen atoms	35291	282408	70604	
Protein residues	2378	19024	4756	
Ligands	16	136	36	
Validation				
R.m.s. deviations				
Bond lengths (Å)	0.008	0.008	0.008	
Bond angles (°)	1.423	1.266	1.256	
Ramachandran plot (%)				
Favored	90.04	90.43	90.15	
Allowed	9.87	9.57	9.77	
Outliers	0.00	0.00	0.08	

Supplementary Table S1. Cryo-EM data collection, refinement and validation for VWF datasets.